ISSN 0016-7932, Geomagnetism and Aeronomy, 2016, Vol. 56, No. 4, pp. 448–456. © Pleiades Publishing, Ltd., 2016.
Original Russian Text © D.V. Blagoveshchenskii, 2016, published in Geomagnetizm i Aeronomiya, 2016, Vol. 56, No. 4, pp. 479–488.

Anomalous Phenomena on HF Radio Paths during Geomagnetic Disturbances

D. V. Blagoveshchenskii

St. Petersburg State University of Aerospace Instrumentation, ul. Bol'shaya Morskaya 67, St. Petersburg, 190000 Russia

e-mail: donatbl@mail.ru

Received November 18, 2015; in final form, January 11, 2016

Abstract—We analyze ionospheric oblique sounding data on three high-latitude and one high-latitude–mid-latitude HF radio paths for February 15 and 16, 2014, when two substorms and one magnetic storm occurred. We investigate cases of anomalous propagation of signals: their reflection from sporadic layer *Es*, lateral reflections, type "M" or "N" modes, the presence of traveling ionospheric disturbances, and the diffusivity of signals and triplets. The most significant results are the following. In geomagnetically undisturbed times, sporadic *Es*-layers with reduced maximum observed frequencies (MOF*Es*) on three high-latitude paths were observed in both days. The values of MOF*Es* during disturbances are large, which leads to the screening of other oblique sounding signals reflected from the ionosphere. On all four paths, the most frequently traveling ionospheric disturbances due to the terminator were observed in quiet hours from 03:00 to 15:00 UT on the first day and from 06:00 to 13:00 UT on the second day of the experiment. In addition, both the sunset terminator and the magnetic storm on the high-latitude–mid-latitude path were found to generate traveling ionospheric disturbances jointly. No such phenomenon was found on high-latitude paths.

DOI: 10.1134/S0016793216040022

1. INTRODUCTION

Geomagnetic disturbances are the principal and major source of the anomalous state of near-Earth space weather. The highest manifestations of disturbed space weather are magnetospheric storms and substorms, which can cause substantial adverse effects on both complex terrestrial and space technological systems. These effects include cases of electricity supply failures in energy networks because of the guidance of strong harmful currents, satellite damage by high-energy particles, the sharply increased risk of human exposure to radiation in space and high-altitude aircrafts, errors in GPS and low-frequency navigation systems, failures in HF communication systems, etc. The geomagnetic disturbances considered below have a natural (solar) origin. They are known to occur primarily in the high-latitude ionosphere; the disturbance effects then shift toward the equator. During disturbances, a substantial restructuring of the ionospheric structure occurs, thus breaking the radiowave propagation conditions.

Anomalous cases of propagation include signal reflections from the sporadic *Es*-layer, lateral reflections, modes of "M" and "N" types, the presence of traveling ionospheric disturbances (TIDs), and the diffusivity of signals and triplets (Blagoveshchenskii, 2011). All of these are anomalous cases, namely with respect to normal propagation along the great circle arc with reflection from the *F*-region. At high latitudes, anomalous propagation is known to be a common phenomenon and naturally causes difficulties in the use of radio channels. In our experiment, the position of radio paths was chosen in such a way that their reflection points are arranged in sequence from north to south in the longitudinal direction. This made it possible to track the dynamics of disturbance effects on the ionosphere and the propagation conditions. This could be done, in concept, with the help of ionosondes. However, the experimental site is in a region where no ionospheric vertical sounding stations are available, and oblique sounding of the ionosphere (OSI) has to be used as a diagnostic tool. It should be noted that problems of HF propagation have been developed at a new quality level (Hunsucker and Hargreaves, 2003); they are of current interest and are important not only from the scientific point of view. Their practical significance stems from the reasonable organization of HF radio communication (for example, when the Arctic shelf is explored for oil extraction) with Northern Sea Route vessels and with aircrafts flying over the Arctic, as well as from the need to solve problems in communication, navigation, and over-the-horizon radiolocation not only at high latitudes. Therefore, it is important to study the adverse impacts of disturbance effects on the radiowave propagation.

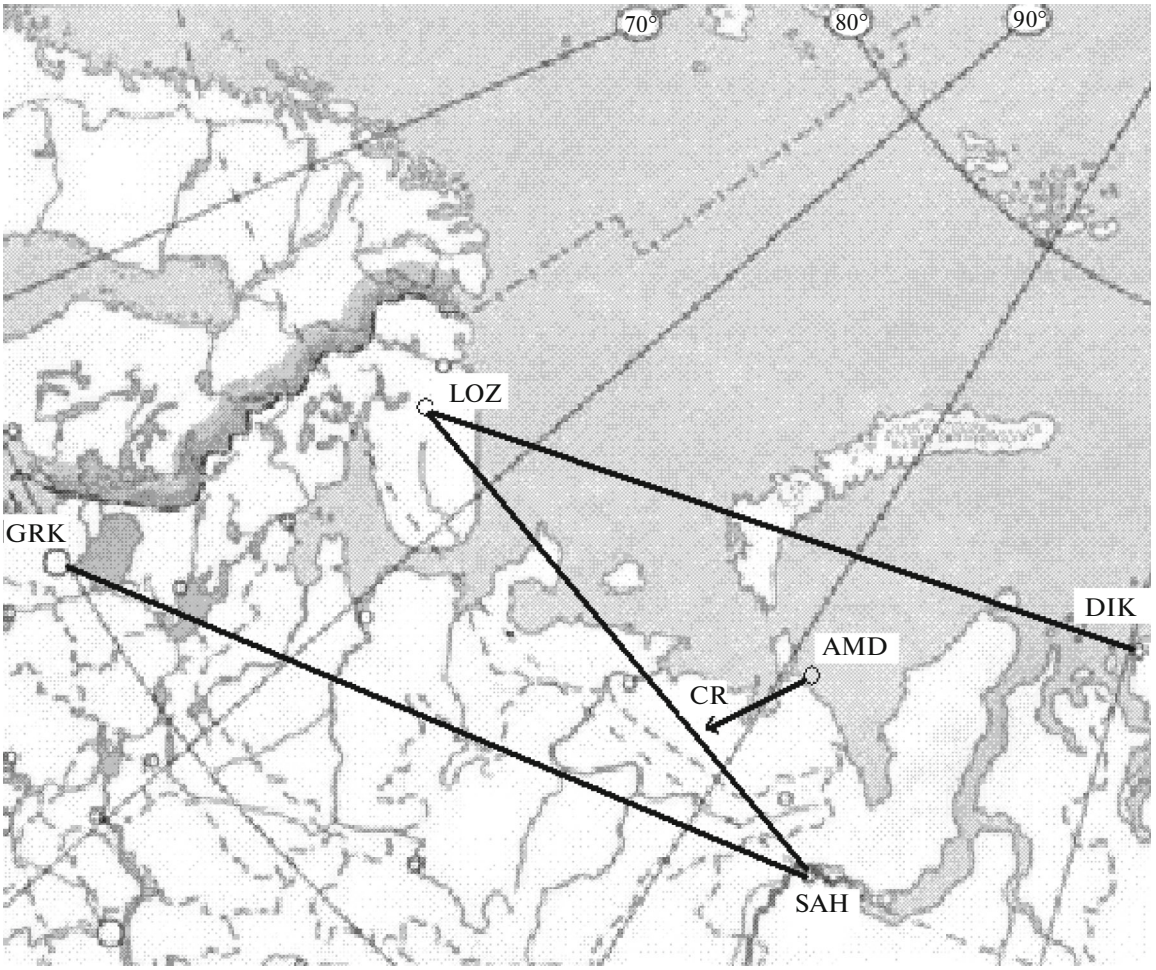

Fig. 1. General schematic of the four radio paths involved in the experiment: Dikson–Lovozero, Salekhard–Lovozero, Salekhard–Gorkovskaya, and Amderma–Cyprus.

This study aims to reveal possible regularities in the behavior of uncommon cases of HF radiowave propagation on three near-polar radio paths and one additional high-latitude–mid-latitude during radio path during geomagnetic disturbances. The observations were conducted on February 15 and 16, 2014, when two substorms and one magnetic storm occurred.

2. DESCRIPTION OF THE EXPERIMENT

Figure 1 shows the schematic of radio paths used in the experiment. These paths are part of the general system of OSI paths of the Arctic and Antarctic Research Institute in St. Petersburg. There are four actually operating radio paths of the general system. The first (northernmost) is the Dikson (DIK)–Lovozero (LOZ) path with a length of 1730 km. Hereafter, the first station in the path name means the transmitter and the second station stands for the receiver. The second (more southern) is the Salekhard (SAH)–Lovozero path with a length of 1355 km. The third (southernmost of the three high-latitude paths) is the Salekhard–Gorkovskaya (GRK) path with a length of 1947 km (the longest). All three are one-hop paths. The final is the Amderma (AMD)–Cyprus (CR) auxiliary radio path with a length of 4165 km, which belongs to the category of high-latitude–mid-latitude paths. Its role is auxiliary because, first, it is only partially of high-latitude and, second, some OSI sessions are not available on it. The coordinates of the terminal stations of all paths are presented in the table. It can be seen from Fig. 1 and the table that the reflection points of high-latitude paths lie nearly along the longitude and are spatially separated by around 4°. This unusual meridional chain makes it possible to conduct a more detailed investigation of processes during the storm/substorms, because these processes proceed differently depending on latitude and local time. The OSI sessions were organized on the paths every 15 minutes on a twenty-four-hour basis. The two days yielded a total of $48 \times 4 = 192$ ionograms per path. The ionograms were used to find anomalous propagation cases to be analyzed. Examples of OSI ionograms are given in Fig. 2, which shows all of the

Geographic and geomagnetic coordinates of OSI receiving–transmitting stations

No.	Code	OSI station	Geographic coordinates, deg.		Geomagnetic coordinates (CGM), deg.	
			latitude, N	longitude, E	latitude, N	longitude, E
1	GRK	Gorkovskaya	60.27	29.38	56.81	105.71
2	LOZ	Lovozero	68.00	35.02	64.64	113.80
3	AMD	Amderma	69.60	60.20	65.87	136.58
4	SAH	Salekhard	66.52	66.67	62.87	141.63
5	DIK	Dikson	73.52	80.68	69.29	156.30
6	Cyprus	Cyprus	35.00	34.00	30.71	112.50

anomalous situations mentioned above; they considered below in greater detail.

As mentioned, February 15 and 16, 2014, were chosen as the disturbance days. The first day was characterized by a weak substorm with a duration of 2.5 h in the daytime hours (13:30–16:00 UT). Its intensity was low and AE_{max} = 350 nT. The second (nighttime) substorm began late in the first day at 23:30 UT and terminated at 02:00 UT of the next day; i.e., its duration was 2.5 h. This substorm was quite intense and characterized AE_{max} = 810 nT. The third outrage is a magnetic storm duration of 7 hours. It started at 15:00 UT and ended late on 22:00 UT February 16, 2014 The storm was sufficiently intense with AE_{max} = 1050 nT. The schematic of all these disturbances are shown in the bottom of Figs. 3–6. It can be seen that the first weak disturbance occurred on a quiet magnetic background, the second (moderate) disturbance occurred on a slightly disturbed background, and third (strong) disturbance occurred on a more perturbed background.

3. DATA ANALYSIS AND DISCUSSION

3.1. Sporadic Es-Layers

It should be noted primarily that the sporadic layers at high latitudes emerge quite regularly rather than sporadically. In the auroral zone, there are three main types of these layers: thick uniform, thick nonuniform, and flat (Razuvaev, 1991). The first two types are caused by the precipitation of charged particles from the magnetosphere. The thick uniform type spatially coincides with the area of diffuse auroral precipitations, and its formation can be associated with both proton and electron precipitations. It is known that the height of the *Es*-layer decreases, its half-thickness reduces, and the electron density at the maximum increases during a substorm. The question arises as to why this study considers the emergence of sporadic layers as an anomalous phenomenon. Our answer is that normal reflections of OSI signals from the *F*2 layer pass to reflections from only sporadic *Es*-layers during geomagnetic storms and substorms. The reflections from the *F*2-layer are screened by reflections from the *Es*-layer, and it is the latter reflection that is observed (an example is shown in Fig. 2, top panel, left).

Figure 3 shows the general pattern of changes in the maximum observed frequency MOF*Es* on three high-latitude paths during the day for February 15–16, 2014. The top panel (a) corresponds to the Dikson–Lovozero high-latitude path. The second panel (b) refers to the Salekhard–Lovozero path. The third (c) panel corresponds to the Salekhard–Gorkovskaya path. The bottom panel (d) shows the magnetic disturbances for these two days. Their intensity is characterized by the *AE*-index. The vertical lines indicate the onset *To* and the end *Te* of a substorm or storm. The black color indicates the most disturbed part of substorm/storm. It can be seen that the first weak substorm (13:30–16:00 UT) causes an increase in MOF*Es* only on the highest-latitude (Dikson–Lovozero) path. On other paths, this effect is absent. This can be physically explained, because a growth in the latitude increases the probability of particle precipitation even at a weak disturbance. Due to their intensity, the second substorm (23:30–02:00 UT) and the magnetic storm (15:00–22:00 UT) cause a growth in MOF*Es* on all the three paths. Now, we consider the assumption on increased values of MOF*Es* on the highest-latitude path from 18:00 to 22:00 UT. According to (Blagoveshchenskii, 2011; Pirog et al., 2000), thick sporadic *Es*-layers with large limiting frequencies *foEs* appear at latitudes of 65° and above a few hours before the substorm onset. Incidentally, these layers can serve as a precursor of substorm development (Blagoveshchenskii, 2011; Pirog *et al.*, 2000). However, this effect refers only to significantly higher latitudes. Figure 3 also shows that, during the geomagnetically undisturbed time interval 04:00–13:00 UT, the sporadic *Es* with decreased *MOFEs* on the three paths are observed on both the first and second days. On the other hand, according to Fig. 3, since the values of MOF*Es* on the given three paths during the disturbances are sufficiently large, it can be expected that other OSI signals with the maximum observed frequency reflected from the ionosphere will be screened by sporadic layers.

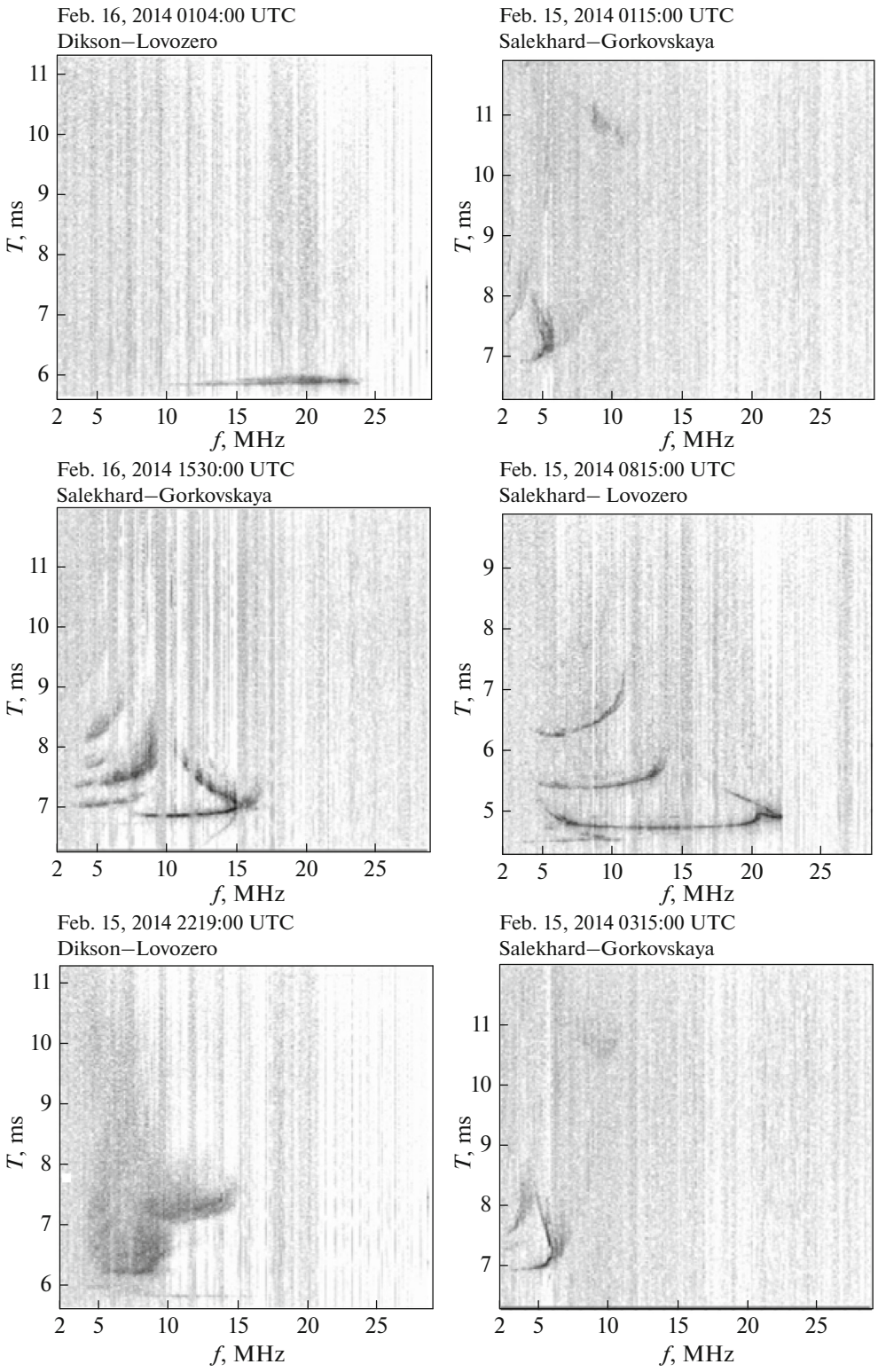

Fig. 2. Examples OSI ionograms for different anomalous situations. Sporadic *Es*-layer; lateral reflection, mode "M" or "N"; TID; diffusivity and triplet (from left to right and down).

3.2. Lateral Reflections

At high latitudes, deviations from the great circle arc (lateral signals) during the propagation of radiowaves are known to be largely caused by variations in electron density in the ionosphere. Namely, the electron density gradients or nonuniformities in its distribution cause a lateral reflection or scattering of signals. The horizontal gradients are large in the center of the

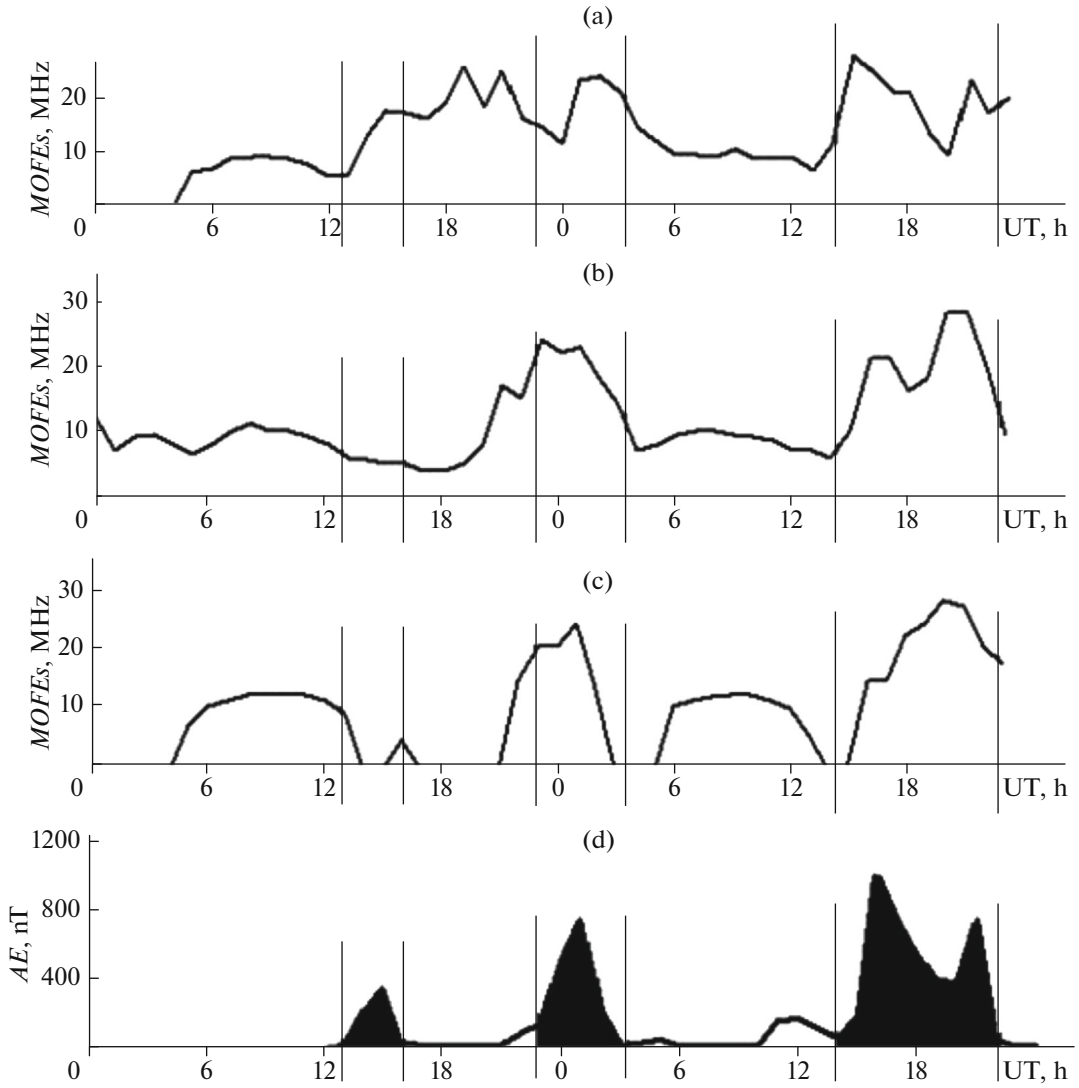

Fig. 3. Variations in MOF*Es* on three paths: (a) Dikson–Lovozero, (b) Salekhard–Lovozero, and (c) Salekhard–Gorkovskaya for February 15–16, 2014. The bottom panel (d) shows the values of *AE*-indices.

auroral oval, on its equatorial boundary that separates the region of intense precipitations of energetic particles and the main ionospheric trough (MIT), in the regions of inflow and outflow of longitudinal currents, and in the area of the daytime cusp. The formation of inhomogeneities and the dynamics of the high-latitude ionosphere are largely determined by a strong external electric field. There can also be different local plasma compressions conditioned by nonuniformity in the intrusion of charged particles or by the internal dynamics of the polar ionosphere. Figure 2 (top panel, right) shows an example of OSI ionogram on the Salekhard–Gorkovskaya path with a lateral reflection. This signal is in the frequency range $f = 9–12$ MHz with a delay of $T = 11$ ms. The lower frequency of this signal $f = 9$ MHz exceeds MOF$F2 = 6$ MHz of the main signal, which is usually satisfied in practice.

Figure 4 shows the variation in the MOF of lateral reflections on three high-latitude radio paths for two days. The bottom panel shows the *AE*-index of magnetic activity. The vertical lines denote the *To* values indicating the onset of disturbance (storm or substorm). It follows from this figure that all paths have lateral reflections with low values of MOF in the quiet night hours of February 15, 2014, from 00:00 to 03:00 UT. This can be caused by the fact that the northern wall of the MIT during these hours is closest to the paths, and the lateral signals are reflected from it. During the disturbances, the pattern is different. The first weak substorm makes a restructuring in the ionosphere, which may include gradients and nonuniformities. This leads to the formation of lateral reflections with high MOF values. During the second intense substorm close to midnight, no lateral reflections are found. Most probably, they do exist but are screened by sporadic layers

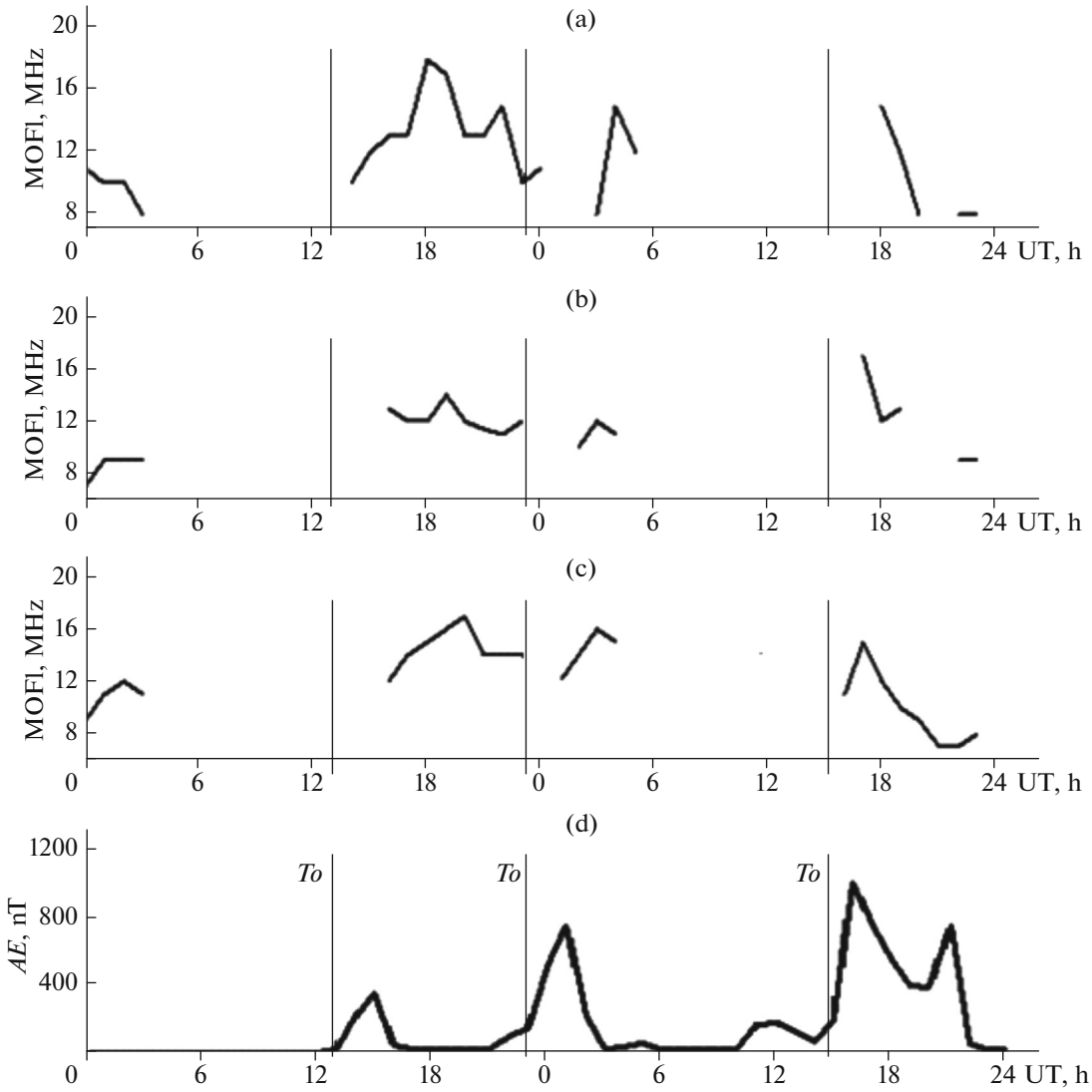

Fig. 4. Same as Fig. 3 except for MOFs of lateral reflections (MOFl).

with large values of MOF*Es* (see Fig. 3). The end of the second substorm is followed by a quiet period, and the lateral signals at 04:00–15:00 UT on February 16, 2014, disappear, almost as on February 15, 2014, in the given time interval. The storm is characterized by lateral reflections, but the sporadic layers partially screen them (see Fig. 3). The screening is especially pronounced for the two northernmost paths (two top panels).

3.3. Anomaly Modes "M" or "N"

At high latitudes, the structure of HF radiowave propagation trajectory is often very complex and includes reflection from several layers (Davis, 1973). For example, it is known that *F* and 2*F* denote one and two reflections from the *F*-region, respectively. The reflection from the Earth is usually denoted by a hyphen. Then, *F*–*F* corresponds to 2*F*. More difficult is the *FEF* path. Here, the signal from the transmitter is first reflected from the *F*2-layer, then from the *E*-layer, and again from *F*2. This trajectory is sometimes called the "M" mode. For *E*–*F*, the first reflection is from the *E*-layer, then from the Earth, and the final reflection is from the *F*2-layer. This trajectory is sometimes called the "N" mode. Figure 2 (middle panel, left) shows an example of anomalous modes for the Salekhard–Gorkovskaya path. The first path in the frequency range $f = 3.5$–8 MHz and with a delay of $T \approx 7$ ms corresponds to one-hop propagation. The second path is in the frequency range $f = 4$–6 MHz and with a delay of $T \approx 7.7$ ms is characterized by two-hop propagation. These anomalous modes can be conditionally compared with normal modes on the Salekhard–Lovozero path (middle panel, right). It can be seen that the right ionogram includes only normal modes, and the anomalous modes (apart from main modes) are found only on the left ionogram.

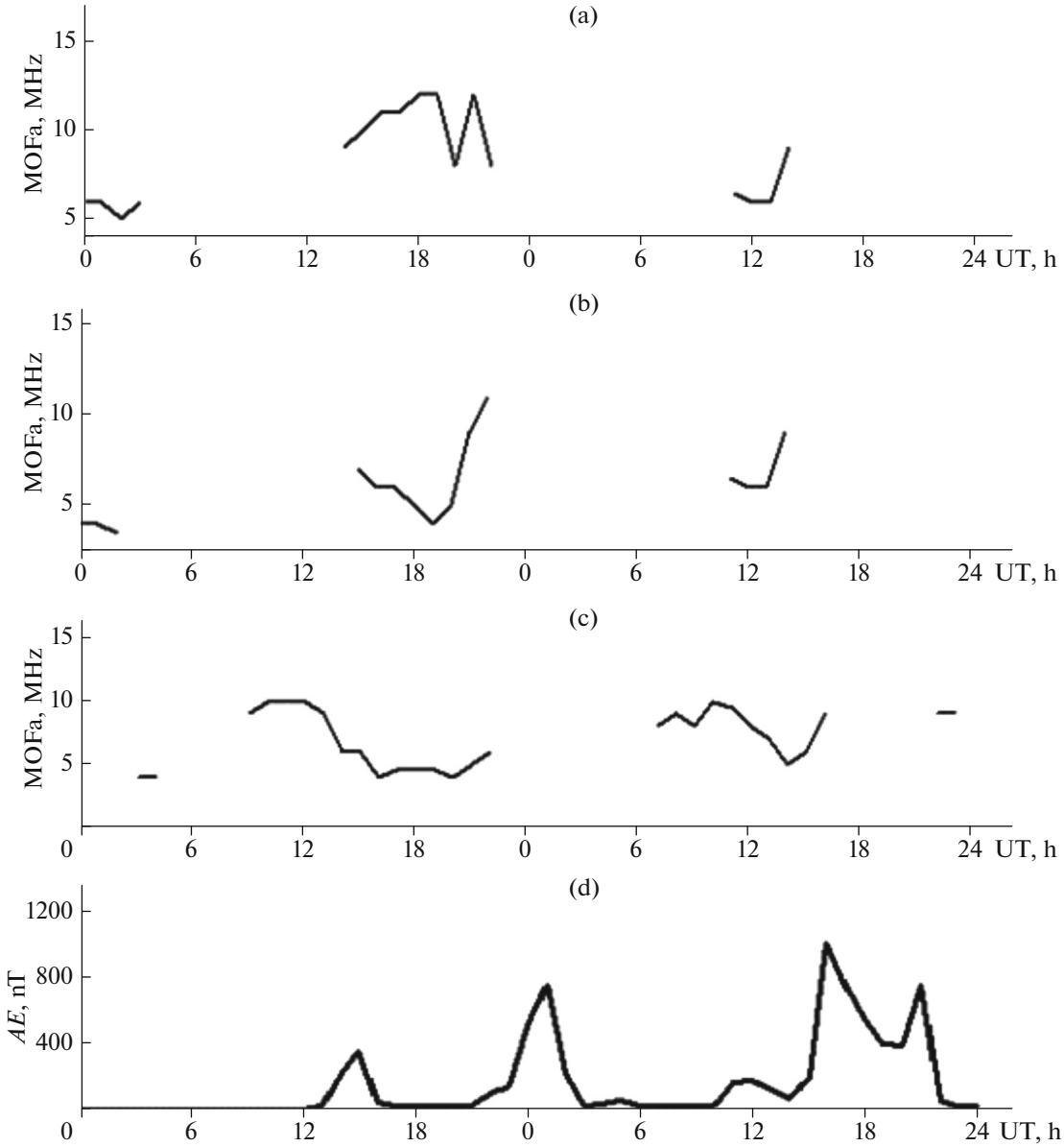

Fig. 5. Same as Fig. 3 except for MOFs of anomalous modes "M" or "N" (MOFa).

Figure 5 shows the temporal variations in the MOF of modes "M" or "N" for February 15–16, 2014. It can be seen that, first, when no disturbances are present, the anomalous modes on all paths are observed only in midnight hours on February 15, 2014. Second, during disturbances, the first substorm (when the ionosphere is modified) is characterized by the emergence of anomalous modes up to the onset of the second substorm. During the second substorm, the paths are most likely characterized by screening of anomalous layers by reflections from sporadic *Es*-layers (see Fig. 3). During the magnetic storm in the evening of February 16, 2014, also according to the supposition, there occurs a screening of anomalous modes by sporadic *Es*-layers. Third, comparison of the path data shows that the total number of occurrences of anomalous modes on the third (southernmost, Salekhard–Gorkovskaya) path is significantly higher than on the first two paths. This can be explained as follows. The Salekhard–Gorkovskaya path is the southernmost of the given three paths. This path is close to the midlatitudes, where the HF radio channels are generally more stable in time, i.e., they exist for a long time at the same parameters. The stability of channels at high latitudes is lower due to different geophysical impacts and are thus highly variable.

3.4. Traveling Ionospheric Disturbances (TIDs)

Traveling ionospheric disturbances (TIDs) are permanently present in the Earth's ionosphere. The role of the terminator in their formation (especially, in sunrise–sunset hours) was a proven fact. For example,

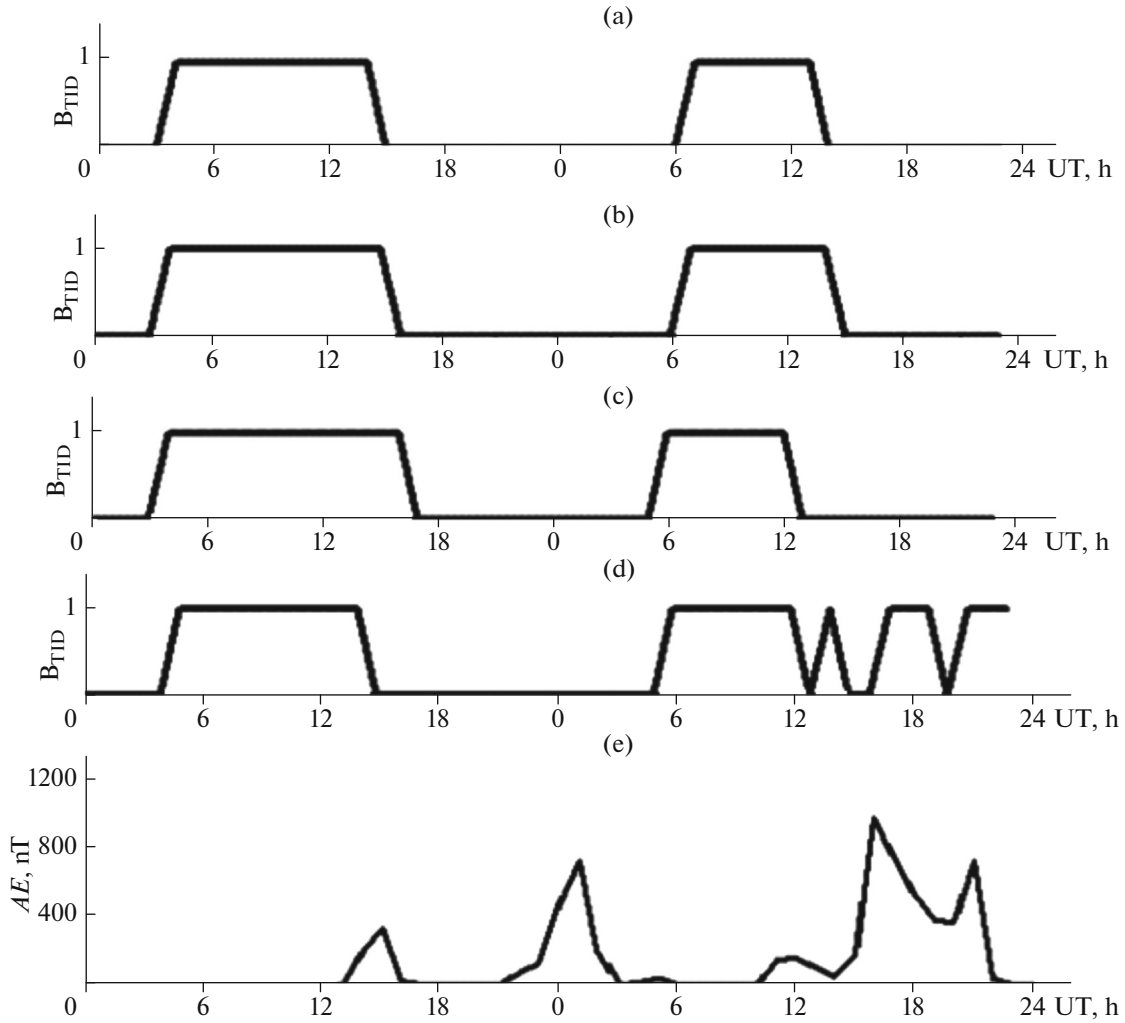

Fig. 6. TID probability (B_{TID}) at four paths: (a) Dikson–Lovozero, (b) Salekhard–Lovozero, (c) Salekhard–Gorkovskaya, and (d) Amderma–Cyprus for February 15–16, 2014. (0) no TIDs and (1) presence of TIDs. The bottom panel (e) shows the values of *AE*-indices.

Vertogradova (2014) showed that TIDs appear on OSI ionograms on the Cyprus–Rostov-on-Don as formations of *z*-shaped patterns or steps. These formations are observed first in the vicinity of the lowest observed frequency (LOF) for upper beams and then travel over time into the region of lower delays (the MOF region). Figure 2 (middle panel, right) shows an example of the *z*-formation that occurred on the high-latitude Salekhard–Lovozero path. It can be seen that the TID affects the mode 1*F*2 (the first jump of the OSI signal) in the vicinity of MOF as a step. Namely, this step is near the frequency $f = 20.5$ MHz. With no traveling disturbance, the step should be absent.

Figure 6 shows the probability of TID occurrence on three high-latitude paths (panels a, b, and c) and one high-latitude–mid-latitude path (panel d). Here, the numbers 1 and 0 indicate the presence and absence of TID, respectively. It follows from the figure that on February 15, 2014, the traveling disturbances due to the terminator observed are most frequent in quiet hours from 03:00 to 15:00 UT. Usually, in mid-February during polar winter in the north, the morning hours actually go to evening hours in terms of illumination. Therefore, the morning and evening terminators for the given conditions practically merge. On the second day, February 16, 2014, the appearance of TIDs is slightly less frequent and lies in the range from 06:00–13:00 UT. The reduction in the interval may be caused by greater magnetic disturbances of this day and violation of the TID formation regime. Figure 6 (panel d) shows data for the Amderma–Cyprus path to emphasize the following factor. MacDougall and Jayachandran (2011) analyzed the probability of TID occurrence at midlatitudes according to ionosonde data (London, Canada, 43° N, 81° W) for 2000 and revealed that the TID is caused by the sunrise terminator. However, in the evening and night hours, the sunset terminator and magnetic disturbances jointly contribute to TID formation. In the case of the evening terminator and the magnetic storm from 15:00 to 22:00 UT, Figure 6d shows the

probability of TID occurrence on the Amderma–Cyprus path. According to the table, the reflection point of this path is located at a latitude of 48° N, which is rather close to the latitude of London 43° N. It can be seen from Fig. 6d that both the sunset terminator and the magnetic storm jointly generate a TID similar to the London (Canada) ionosonde data. At high-latitude paths, no phenomenon of this kind is found.

3.5. Diffusivity

Diffusivity almost always occurs on all high-latitude paths, especially during geomagnetic disturbances. Actually, the degree of diffusivity cannot be quantitatively estimated; it can be estimated only qualitatively (significant, weak, or absent). An example of significant diffusivity is shown in Fig. 2 (bottom panel, left). Here, it is very difficult to estimate the TID value for the paths of signals.

3.6. Triplets

It is known that the ionograms of vertical ionospheric sounding sometimes may have three rather than two reflected waves: one ordinary and two extraordinary waves; i.e., a triplet (instead of a doublet) of reflected signals is received (Alpert, 1972). This leads to the appearance of the third branch on altitude–frequency characteristics. The three branches are predominantly observed at high latitudes in the *F*-field and less often in the *E*-region. Under some conditions, these characteristics can also be observed at midlatitudes. Figure 2 (lower panel, right) shows an example of a triplet for the high-latitude Salekhard–Gorkovskaya path. Here, we have MOF = 7 MHz on the one-hop mode 1*F*2. In our experiment, such cases of triplets are rare; therefore, no statistics is available for them.

4. CONCLUSIONS

OSI data were analyzed on three high-latitude and one high-latitude–mid-latitude HF radio paths for February 15 and 16, 2014, when two substorms and one magnetic storm occurred. The position of radio paths was chosen in such a way that their reflection points are arranged in sequence from north to south in the longitudinal direction. This unusual meridional chain makes it possible to conduct a more detailed investigation of processes during a storm/substorm, because these processes proceed differently depending on latitude and local time. Consequently, this made it possible to track the dynamics of disturbance effects on the ionosphere and the propagation conditions. The following key results were obtained.

(1) In a geomagnetically undisturbed time, (a) the three high-latitude paths have lateral reflections possibly from the northern wall of the MIT, with low values of MOF; (b) anomalous modes "M" or "N" are observed on the paths only in midnight hours; and (c) sporadic *Es*-layers with decreased MOF*Es* on three high-latitude paths are observed in both the first and second days. On the other hand, because the MOF*Es* values on the given three paths during the disturbances are sufficiently large, it can be expected that other OSI signals with a lower MOF reflected from the ionosphere will be screened by sporadic layers.

(2) On all four paths, the most frequently traveling ionospheric disturbances due to the terminator were observed in quiet hours from 03:00 to 15:00 UT on the first day and from 06:00 to 13:00 UT (slightly shorter than on the first day) on the second day. This is caused by the fact that, in mid-February during polar winter in the north, the morning hours actually go to evening hours in terms of illumination. Therefore, the morning and evening terminators for the given conditions practically merge. Also, we have found that on the high-latitude–mid-latitude path, the sunset terminator and the magnetic storm jointly generate TIDs. On high-latitude paths, no such phenomenon can be found.

ACKNOWLEDGMENTS

The author is highly grateful to the Sodankylä Observatory and Kyoto Data Center for the opportunity to use their geophysical data available on the Internet, as well as to D.D. Rogov, a scholar at the Arctic and Antarctic Research Institute in St. Petersburg, for providing ith ionospheric oblique sounding data.

This study was supported by the Russian Foundation for Basic Research, project no. 15-05-00856.

REFERENCES

Al'pert, Ya.L., *Rasprostranenie elektromagnitnykh voln i ionosfera* (Propagation of Electromagnetic Waves in the Ionosphere), Moscow: Nauka, 1972.

Blagoveshchenskii, D.V., *Short Waves in Anomalous Radio Channels*, Saarbrücken, Germany: LAP Lambert, 2011.

Davies, K., *Ionospheric Radio Waves*, Waltham, MA: Blaisdell, 1969; Moscow: Mir, 1973.

Hunsucker, R.D. and Hargreaves, J.K., *The High-Latitude Ionosphere and Its Effects on Radio Propagation*, Cambridge University Press, 2003.

MacDougall, J.W. and Jayachandran, P.T., Solar terminator and auroral sources for traveling ionospheric disturbances in the midlatitude *F* region, *J. Atmos. Sol.–Terr. Phys.*, 2011, vol. 73, no. 11, pp. 2437–2443. doi 10.1016/j.jastp.2011.10.009

Pirog, O.M., Urbanovich, V.D., and Zherebtsov, G.A., Effects of substorms in the night auroral *E*-region, in *Proceedings of the 5th International Conference on Substorms*, St. Petersburg, 2000, pp. 545–547.

Razuvaev, O.I., Sporadic ionization in high-latitude geophysical studies, in *Issledovaniya po geomagnetizmu, aeronomii i fizike Solntsa* (Studies on Geomagnetism, Aeronomy, amd Solar Physics), Moscow: Nauka, 1991, vol. 93, pp. 3–16.

Vertogradova, E.G., Diagnostics, modeling, and prediction of the characteristics of decameter radio waves in naturally disturbed and artificially modified ionosphere, *Cand. Sci. (Phys.–Math.) Dissertation*, Rostov-on-Don: Southern Federal University, 2014.

Translated by V. Arutyunyan